Molecular and Mechanical Properties of Major Ampullate Silk of the Black Widow Spider, Latrodectus h esperus

3 AUTHORS, INCLUDING:

Craig A Vierra

University of the Pacific (California - USA)

27 PUBLICATIONS **539** CITATIONS

Molecular and Mechanical Properties of Major Ampullate Silk of the Black Widow Spider, *Latrodectus hesperus*

Barbara A. Lawrence,*,[†] Craig A. Vierra,[‡] and Anne M. F. Moore[‡]

*Department of Chemistry, Eastern Illinois University, Charleston, Illinois 61920, and
Department of Biological Sciences, University of the Pacific, Stockton, California 95204*

Molecular and material properties of major ampullate silk were studied for the cobweb-building black widow spider *Latrodectus hesperus*. Material properties were measured by stretching the silk to breaking. The strength was 1.0 ± 0.2 GPa, and the extensibility was 34 ± 8%. The secondary structure of the major ampullate silk protein was studied using carbon-13 NMR spectroscopy. Alanine undergoes a transition from a coiled structure in pre-spun silk to a beta sheet structure in post-spun silk. We have also isolated two distinct cDNAs (both about 500 bp) which encode proteins similar to major ampullate spidroin 1 and 2 (MaSp1 and MaSp2). The MaSp1-like silk contains polyalanine runs of 5−10 residues as well as GA and GGX motifs. The MaSp2-like silk contains polyalanine runs of varying length as well as GPG(X)$_n$ motifs. *L. hesperus* major ampullate silk is more like major ampullate silk from other species than other *L. hesperus* silks.

Introduction

Major ampullate (MA) silks produced by orb web spiders from the genera *Nephila* and *Araneus* have been the subject of detailed study because of their exceptional material properties.[1,2] Major ampullate silk is utilized in the orb web as the structural radial threads as well as the major component (along with minor ampullate silk) of the dragline, the thread by which the spider suspends itself. Orb web MA silk consists of two large molecular weight proteins: spidroin 1 (MaSp1) and spidroin 2 (MaSp2).[3,4] The principle amino acids in both *Nephila* and *Araneus* MA silks are glycine, alanine, and glutamine.[5,6] The established structure of MA silk is that of a block copolymer: small polyalanine crystallites in antiparallel beta sheet configuration[7] embedded in a glycine-rich matrix. The crystalline regions have been associated with the high strength of MA silk and the surrounding matrix with extensibility. Different structures for the matrix have been proposed for *Araneus* and *Nephila* MA silk. For *A. diadematus* MA silk, glycine-rich amorphous chains connecting the crystals have been proposed[2] as a simple model to account for material properties of both dry and hydrated silk. On the other hand, two-dimensional NMR experiments on *N. clavipes* MA silk have revealed a higher-order, 3$_1$-helix conformation in the glycine-rich region.[8,9]

Many orb-web spiders produce six or more silks[10] in addition to major ampullate silk, each with a specific function such as prey capture or egg protection.[11] Although major ampullate silk has been studied in the greatest detail, other orb web silks have been studied and shown to exhibit very different properties.[12] Although MA silk from orb weavers *Nephila* and *Araneus* exhibit differences in material proper-

ties and molecular structure, they are strikingly similar when compared to other silks from the same spiders. For instance, flagelliform silk (the base silk of the capture spiral) has lower tensile strength and greater extensibility than MA silk.[12]

There have been few detailed studies of mechanical and molecular properties of silk from spiders that construct nonorb webs.[13] The black widow spider *Latrodectus hesperus*, a member of the family Theridiidae, constructs a cobweb with gumfoot lines. The theridiid cobweb is thought to be homologous to orb webs,[14] but is structurally distinct. The *Latrodectus* cobweb functions differently from an orb web. The cobweb itself consists entirely of scaffolding silk[15] and gumfoot silk.[16] MA silk has not been found in a *Latrodectus* web;[17] unlike orb web MA, the only function that MA silk serves in the cobweb is in the dragline. Thus, the only function that MA silk shares in all three, *Nephila*, *Araneus*, and *Latrodectus,* is that of holding the weight of the spider as a dragline. Previous work[17] has revealed that *Latrodectus* MA silk consists of two large molecular weight proteins with amino acid concentrations similar to other MA silks: glycine (42%), alanine (27%), and glutamine (12%) being the three main components.

We are reporting the results of a multi-disciplinary study of MA silk from the black widow spider, *L. hesperus*. We have studied the material properties of the silk using a stress−stain analysis and the secondary structure of the silk using carbon-13 NMR. In addition, we have analyzed the genes that encode the silk protein. We compare and contrast the properties of *L. hesperus* dragline silk with those of the MA silks of spiders from the well-studied genera *Araneus* and *Nephila*.

Experimental Section

Spider Care. Approximately 100 adult female black widows (*Latrodectus hesperus*) were collected in San Joaquin

---

* To whom correspondence should be addressed. Phone: 217-581-2720. E-mail: cfbal1@eiu.edu.
† Eastern Illinois University.
‡ University of the Pacific.

County, California. Spiders were housed separately in 22 × 40 × 30 cm aquarium tanks with a 14 × 18 × 25 cm wooden frame inserted to aid web construction. Spiders were fed one large cricket weekly; being desert organisms, they do not require additional water. Our previously published safety procedures were followed whenever handling the black widows.[18]

Material Property Measurements. Dragline silk was collected for material property measurement by gravity silking: As the spider dropped to the floor, the dragline was reeled (at approximately 2.5 cm/s) onto a 10−15 cm wide cardboard fork. After reeling, single strands of dragline were gently attached to 5 cm Plexiglas forks with double-sided tape. The strand was gently cut (taking care not to stretch the silk) with micro-dissecting scissors to excise it from the cardboard fork. The strand was taken immediately to a dissecting microscope, where the two major ampullate strands were separated. Because dragline silk consists of two large, core fibers of major ampullate silk and two small fibers of minor ampullate silk, small lengths of MA threads were separated so that single fibers could be tested. Under the microscope, the dragline was examined until a slight separation of the two major ampullate strands was found. A small insect pin was inserted into this separation which widened the space between the MA strands. The opening was gradually increased along the entire length of the thread. During this operation, one MA strand was distorted while care was taken to leave the other one unchanged. Minor ampullate strands were easily broken during this operation. Once the two MA strands were completely separated, the distorted strand was cut away from the fork, and the undistorted strand was taken immediately to the micro-tensiometer for mechanical analysis. Thus, there was no fiber damage on MA strands tested.

A silk sample (1−2 cm in length) was glued with cyanoacrylate glue to our micro-tensiometer. The micro-tensiometer consisted of an Aurorascientific 400A force transducer on one side and an Aurorascientific 318B muscle length controller with a 20 mm excursion on the other side. The force transducer could measure forces from 0 to 50 mN to within 1 μN. The length controller could control displacement to within a 1.2 μm and measure displacement with a response time of 500 μs. LabVIEW 5.1 on an IBM platform was used to control the lever arm and to record force and displacement.

Once the glue had dried, the adjacent length of silk was collected on an SEM stub and the fork was gently cut away from the tensiometer with micro-dissection scissors. The distance between mounting pins was then shortened by 1 mm to release any residual tension and ensure data collection at the lowest of stresses. The gage (original) length was measured through a 6× lens to the nearest 0.1 mm. The mounted silk sample was then pulled to the breaking point at a slow speed (0.211 mm/s or strain rate of $0.01-0.02$ s^{-1}) while the force and extension was measured every 11 ms. After the test, broken ends were mounted on a SEM stub. Threads that broke at the grips were discounted. Tests were done under ambient temperature and humidity, which ranged from 20 to 23 °C and 30−36% respectively.

MA silk diameters were measured under a Hitachi S-2600 SEM. Carbon conductive tabs were used to secure the silk to the stub. A hole was punched in the middle of the tab and the silk positioned across the hole so that the middle part of the silk never touched the adhesive of the tab. The samples were coated with a 14−20 nm thick layer of gold in a Pelco SC-7 auto-sputter coater with FTM-2 film thickness monitor. The diameter of both the adjacent and broken strands were each measured at three distant places along the 1−2 cm SEM sample to the nearest 0.1 μm. For most of the samples, the mean diameters of adjacent and broken strands were identical to the nearest 0.1 μm. When there was a difference, it was well within the small, natural variation of diameters found in these threads (see below). When the actual fracture site could be found on the broken strands, the fracture plane was abrupt and perpendicular to the fiber axis. There was no change in diameter in the thread near the fracture site, suggesting that the fiber snapped back to its original shape when the tension was released at breaking. We chose to use the broken strand diameter measurements to compute a circular cross-sectional area because these diameters were closer to the site of fracture.

The force and extension data were used, along with the gage length of the thread and its original cross-sectional area, to construct a stress−strain curve for each sample. Strain was computed by dividing the instantaneous extension by the original length of the thread. Stress was computed as the instantaneous force over the original cross-sectional area.

Six material properties were obtained from the stress−strain curves: Strength, or breaking stress, is the highest stress generated before the thread broke. Extensibility, or breaking strain, is the highest strain generated before the thread broke. Yield stress and yield strain are defined by the point where the curve suddenly changed its slope. The two different slopes constitute pre-yield stiffness and post-yield stiffness. The slopes of these regions were computed by linear regression in SPSS 10.0.

Acquisition of NMR Spectra. MA silk for solid-state NMR analysis was collected as reported in the literature.[19] The spiders were anesthetized with carbon dioxide and pinned down with a barrier designed to protect the collector. After waiting a previously determined[18] recovery time, the silk was collected at a rate of 2.5 cm/s. Collection took place under a microscope to ensure collection of silk from only the MA spinneret. A ^{13}C spectrum of 25 mg of solid silk was obtained on a Bruker AC250 spectrometer equipped with a CP/MAS probe operating at 62.903 MHz. The sample was spun at the magic angle at a rate of 5 kHz. High-power decoupling was used and a contact time of 2.5 s was chosen to match the Hartmann−Hahn condition. The number of acquisitions was 33 000. Chemical shifts were set using an external adamantane standard and referenced to TMS.

Twenty MA glands were carefully dissected from 10 spiders. The intact glands were placed directly into a 5 mm NMR tube filled with a phosphate buffer prepared with 10% D$_2$O for spectrometer locking adjusted to a pH of 7.5. A ^{13}C NMR solution spectrum of the intact glands was obtained with proton decoupling on a Bruker QE300 spectrometer operating at 75.608 MHz. The number of acquisitions was
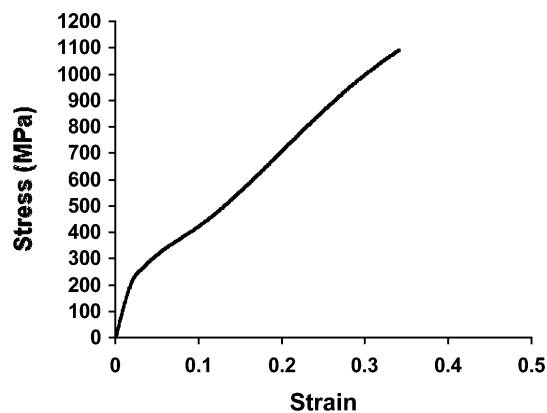
Figure 1. Stress-strain curve for *Latrodectus hesperus*. The curve shows a typical shape for MA silk with an initial stiff region followed by a yield point around 0.02 strain and a combined high strength and high extensibility.

Table 1. Mean (±s.d.) Mechanical Properties of *Latrodectus hesperus* Compared with Values for *Araneus diadematus* and *Nephila clavipes*

	$\sigma_f{}^a$ (MPa)	$\epsilon_f{}^b$ (%)	$E_i{}^c$ (GPa)	$E_f{}^d$ (GPa)
L. hesperus	1000 ± 200	34 ± 8	11 ± 1	2.7 ± 0.7
A. diadematus[e]	1000 ± 300	34 ± 11	6.8 ± 3	3.3 ± 1.8
N. Clavipes[e]	870 ± 350	17 ± 5	11 ± 5	N/R

[a] Strength (σ_f). [b] Extensibility (ϵ_f). [c] Pre-yield stiffness (E_i). [d] Post-yield stiffness (E_f). [e] See ref 25.

12 000 with a 5.0 s delay. Chemical shifts were referenced using an external methanol sample and converted to ppm from TMS. All spectra were analyzed using an NMR analysis program (NUTS) from AcornNMR. Relative peak areas were determined using a deconvolution subroutine in NUTS.

Construction of the cDNA Library. Silk glands were dissected from euthanized *Latrodectus* spiders and these samples flash-frozen immediately in liquid nitrogen. Fifteen spiders were dissected and the following glands were used for the construction of the cDNA library: major ampullate, minor ampullate, flagelliform, tubulliform, aggregate, pyriform, and aciniform. Total RNA was recovered using an RNeasy Maxi kit (Qiagen), followed by the purification of mRNA with a polyATtract mRNA isolation system I kit (Promega). Both procedures were performed according to the manufacturer's instructions. PolyA RNA was converted into double-stranded nucleic acid using a cDNA synthesis kit (Stratagene) and the products ligated into the yeast two-hybrid system cloning vector HybridZap2.1 according to the manufacturer's instructions (Stratagene).

Isolation of the Major Spidroin 1 and 2 Clones. Silk cDNAs were isolated by using anchored PCR. The methodology was as follows: cDNA pieces encoding for MaSp1 and MaSp2 were obtained by PCR using reverse primers designed against a conserved five amino acid region found within the fibroins. Anchored PCR reactions were performed with the cDNA library using the vector-specific forward primer (5′-GCACAGTTGAAGTGAACTTGC-3′) combined with the MaSp1 reverse primer (5′-YTGNCCNGCNC-CNCC-3′) or MaSp2 reverse primer (5′-NGGNCCYTGYT-GNCC-3′). Following amplification, PCR products were ligated into the cloning vector pcDNA3.1/V5−His TOPO (Invitrogen), and the cDNA inserts were analyzed by DNA sequencing (DNA sequencing core facility, University of Florida). Two clones, dubbed MaSp2 and MaSp1, carried cDNAs encoding proteins with motifs similar to other MaSp1 and MaSp2 proteins reported from other species.[20]

Results and Discussion

Material Properties. An example of a stress−strain curve for *L. hesperus* MA silk can be found in Figure 1. The shape

and magnitude of this curve is more similar to that of MA silk in orb-weaving species than it is to *L. hesperus*' own scaffolding silk.[15] *L. hesperus* MA silk shows a characteristic yield point at about 0.024 ± 0.001 strain and 230 ± 30 MPa stress (mean ± standard deviation). Its initial stiffness is 11 ± 1 Gpa, whereas stiffness in the post-yield region is 2.7 ± 0.7 GPa. The post-yield stiffness was measured around 20% strain, well after any yield transition behavior. The post-yield region was considered linear because R^2 values ranged from 0.997 to 0.999 and were always equal to or greater than the R^2 value for the pre-yield region in the same sample. The strength (1.0 ± 0.2 GPa) is comparable to other MA silks, and the extensibility (34 ± 0.9%) is equivalent to *Araneus* but greater than *Nephila*. Table 1 shows mechanical properties measured for *L. hesperus* MA silk and compares them to values for *Nephila clavipes* and *Araneus diadematus* MA silk. Although there have been several studies[21−23] that measured mechanical properties of the latter two silks, the environmental and initial conditions vary from lab to lab because there is no standardized method for testing spider silk.[24] We compare our results to those reported by Work[25] because Work's testing conditions are most similar to ours. The strain rate is identical to our strain rate and they had comparable ranges of temperature and humidity to this study. The values reported here from Work's study come from samples taken directly from orb webs, which is impossible in *Latrodectus* as they do not use MA silk in their webs.

The diameter (3.3 ± 0.8 μm) of MA threads sometimes varies considerably from one thread to the next, but little along a single thread. On some, but not all, MA threads tested, there was a small but significant difference in diameter at different sites along a length. An ANOVA ($p = 0.05$) test of 10 diameter measurements at each of five distant sites along a 2.5 cm strand of MA silk showed small but significant differences in diameter size among sites. The largest difference on any one thread was never more than ±2.5% of the average diameter of the thread. When there was a change in diameter, it did not correlate with the angle of projection of the thread as it twisted, so it is not due to ellipticity of the cross-section. Therefore, the cross-section of MA threads is circular. This is an important distinction as we assumed a circular cross-section to compute the area from the diameter. If the cross-section has more than 20% ellipticity, circular area calculations would introduce a large artifact into our reported stress and stiffness values. Confirmation that the cross-section is indeed circular validates our method.

Although there are clear differences in the material properties of MA silk among species, the magnitude of those differences is equivalent to or lower than the magnitude of
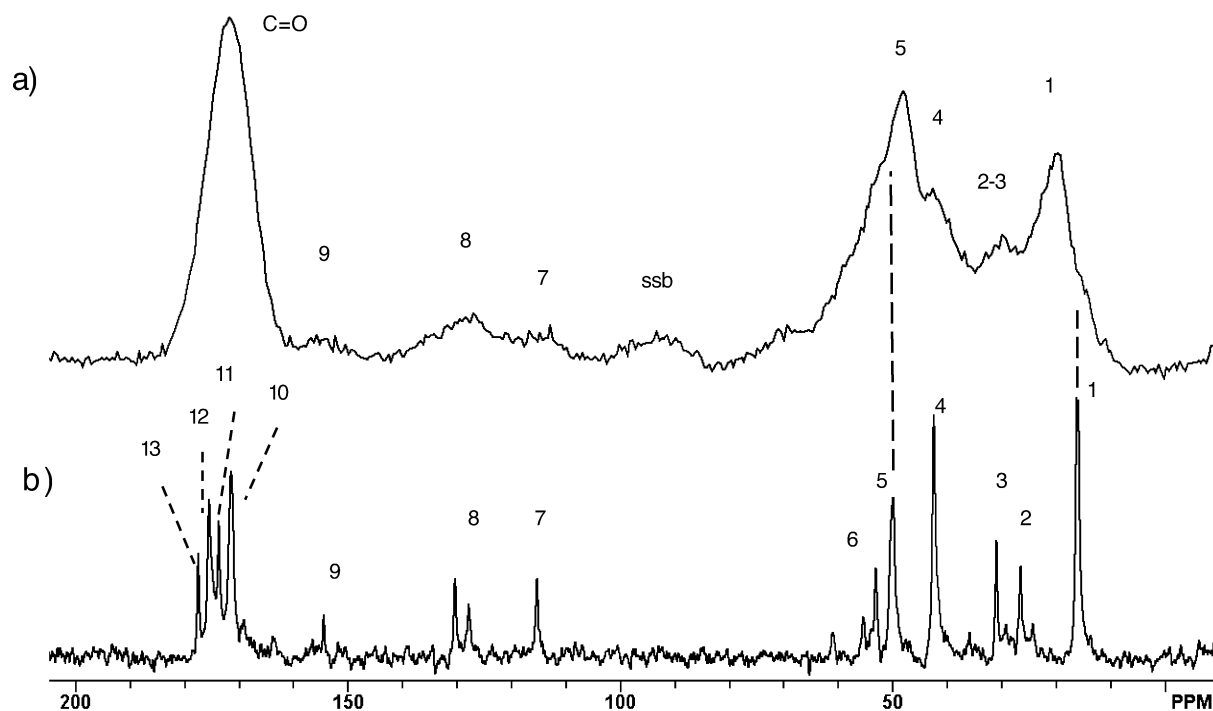
Figure 2. ^{13}C NMR spectra of (a) solid, spun silk and (b) pre-spun silk protein in the major ampullate gland. Assignments are as follows: (1) AlaC$_\beta$, (2) GlnC$_\beta$, (3) GlnC$_\gamma$, (4) GlyC$_\alpha$, (5) AlaC$_\alpha$, (6) SerC$_{\alpha,\beta}$ and GlnC$_\alpha$, (7) TyrC$_\epsilon$, (8) TyrC$_{\delta,\gamma}$, (9) TyrC$_\zeta$, (10) GlyC$_{C=O}$, (11) GlnC$_{C=O}$, (12) AlaC$_{C=O}$, (13) GlnC$_\delta$. A spinning sideband in the CP/MAS spectrum is denoted by ssb.

effects on those same properties due to different strain rates,[2] food intake,[22] and different methods of silking.[26] These MA silks show more mechanical similarity to each other than any one of them shows to another silk produced by a different gland in the same species. Just as MA silk and scaffolding silk in *Latrodectus* have very different stress−strain curves,[15] so do MA silk and flagelliform silk in *Araneus*.[27]

Secondary Structure. Carbon-13 NMR spectra of the spun MA solid silk and of the silk protein in the intact MA gland are shown in Figure 2, parts a and b, respectively. Peak assignments were made using published values for known polypeptides[28] and spider silk.[29] The peaks in the CP/MAS spectrum (Figure 2a) are characteristically broad. The narrowness of the peaks in the gland spectrum (Figure 2b) confirms that the silk protein is in an environment that allows fast segmental motions.[30] Highly immobilized species, for instance lipids in membranes, usually give very broad signals that are invisible in solution NMR or appear as a broad background. The area under the peaks (determined by deconvolution) for both spectra corresponds roughly to the mole percent amino acids previously reported for *L. hesperus* MA silk.[17] However, long ^{13}C relaxation times and differences in cross-polarization efficiency mean that integrated ^{13}C peak areas for either solution or CP/MAS spectra can be considered only estimates.

It has been established that the ^{13}C chemical shifts of the α, β, and carbonyl carbons are dependent not on amino acid sequence but on the conformation of the protein backbone.[28,31] This chemical shift dependence has allowed the use of NMR to determine the secondary structure of amino acids in silkworm silk[32] and Nephila MA silk.[33] If an amino acid is found in more than one specific conformation, the

Table 2. Chemical Shifts (in ppm from TMS) for Polyalanine Carbons in Different Secondary Structures and for *L. hesperus* MA Silk Both Spun and Gland Silk Protein

	random				MA spun silk	MA gland silk
	α-helix[a]	coil[a]	β-sheet[a]	3_1-helix[a]		
Ala C$_\beta$	15.1	17.1	20.1	17.4	20.3	16.1
Ala C$_\alpha$	52.5	50.6	48.7	48.7	48.7	50.2
Ala C$_{C=O}$	176.0	175.2	171.9	172.1	171.8	175.5

[a] References 28 and 31.

resulting chemical shift dispersion will cause line broadening. Alanine exhibits an especially large change in chemical shift with secondary structure; there is, for instance, a 4−5 ppm difference in chemical shift for all three alanine carbons between α-helix and β-sheet structures. Table 2 compares the chemical shifts for polyalanine in four different secondary structures with our results for *L. hesperus* MA silk in the gland and in the spun silk. The alanine alpha and beta carbons (Peaks 1 and 5, Figure 2a) for the spun silk fiber have chemical shifts that are within experimental error of the chemical shifts of the polypeptide beta sheet. These results indicate that alanine in the spun MA silk is found primarily in a β-sheet environment. The best deconvolution fit to the spectrum in Figure 2a reveals a shoulder on the right side of peak 1 at a chemical shift of 16.0 ppm with approximately 5% of the area of peak 1. This chemical shift is 4.0 ppm away from that for an alanine β-carbon in a β-sheet conformation, but within 0.5 ppm of α-helix and random coil chemical shifts. We conclude, therefore, that the alanines represented by this small peak are in a non-β-sheet environment. Because the chemical shift dispersion for the carbonyl carbons is smaller that the peak width for the CPMAS

spectrum, all carbonyl peaks appear under one broad peak (171.8 ppm) and a specific shift for the Ala $C_{C=O}$ cannot be determined.

In the ^{13}C spectrum of the intact glands (Figure 2b), the chemical shifts for the alanine α-carbon (peak 5, 48.7 ppm) and the carbonyl carbon (peak 12, 175.5 ppm) are within experimental uncertainty of the random coil shifts, whereas the beta carbon (peak 1) is midway between random coil and α-helix. The secondary structure of alanine in the pre-spun silk cannot be definitively determined from our data, but it is likely in a coiled structure.

A comparison of the alanine chemical shifts in the pre-spun silk with those in the post-spun silk (see vertical lines at peaks 1 and 5 in Figure 2) reveals that the chemical shifts of the alpha and beta carbons change from those associated with a coiled structure (in the pre-spun silk) to those associated with a β-sheet structure (in the spun silk). Although the chemical shift of the alanine carbonyl peak cannot be determined in the CP/MAS spectrum, as previously discussed, the position of the maximum of the C=O peak is to the right of the envelope of individual peaks in the gland spectrum (Figure 2b, peaks 10−12). This could be the result of a shift to the right of the Ala $C_{C=O}$ from the gland spectrum to the CP/MAS spectrum and would reinforce the conclusion that the alanine residues are in a coiled conformation in the gland and a β-sheet conformation in the spun silk. Thus, our results show that the silk protein undergoes a drastic change in secondary structure between the pre-spun and post-spun silk. It is during this process that the polyalanine beta sheet crystals responsible for the great strength of dragline silk are formed.

These NMR results are similar to results observed for the major ampullate silk of *Nephila clavipes*, in the solid state[33] and in the gland.[34] They stand in contrast, however, to results from the study of post-spun *N. clavipes* minor ampullate (MI) silk,[35] with approximately the same mole percent alanine but only half of the alanines in β-sheet form. Thus, in these cases, there is a greater difference between silk from different glands in the same spider than from silk from the same gland in a different species that builds a different type of web.

Determined Protein Sequence. The peptide from the major ampullate spidroin 1 sequence of *Nephila clavipes*, Gly-Ala-Gly-Gln-Gly (GAGQG), as well as the peptide sequence from major ampullate spidroin 2, Gly-Gln-Gln-Gly-Pro (GQQGP), were used to design reverse DNA primers (5′-YTGNCCNGCNCCNCC-3′ and 5′-NGGNC-CYTGYTGNCC-3′ for MaSp1 and MaSp2, respectively [N = A, C, G, T and Y = C, T] for use in anchored PCR. These peptide regions were selected because of their high conservation in other reported MA silks from a variety of different species.[13] After the completion of anchored PCR, the samples were analyzed by agarose gel electrophoresis and the amplified products visualized by staining with ethidium bromide. cDNAs ranging in size from 300 to 700 bp were excised from the gel and subcloned into the cloning vehicle pcDNA3.1/V5−His TOPO. Several recombinant plasmids carrying amplified products were subject to sequencing. Following sequencing, the nontemplate strand was converted into a protein sequence using the translate program at
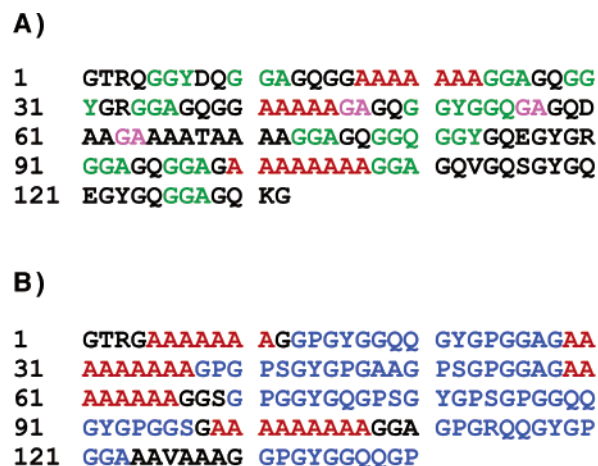
A)

```
1    GTRQGGYDQG GAGQGGAAAA AAAGGAGQGG
31   YGRGGAGQGG AAAAAGAGQG GYGGQGAGQD
61   AAGAAAATAA AAGGAGQGGQ GGYGQEGYGR
91   GGAGQGGAGA AAAAAAAGGA GQVGQSGYGQ
121  EGYGQGGAGQ KG
```

B)

```
1    GTRGAAAAAA AGGPGYGGQQ GYGPGGAGAA
31   AAAAAAAGPG PSGYGPGAAG PSGPGGAGAA
61   AAAAAAGGSG PGGYGQGPSG YGPSGPGGQQ
91   GYGPGGSGAA AAAAAAAGGA GPGRQQGYGP
121  GGAAAVAAAG GPGYGGQQGP
```

Figure 3. Predicted amino acid sequences for the *L. hesperus* spidroins after translation of the nontemplate cDNA strand using the computer program translate at ExPASy. Single letter symbols representing the twenty amino acids are used and GGX, GA, A_n, and $GPG(X)_n$ motifs are indicated in green, pink, red, and blue, respectively. (A) MaSp1-like protein. (B) MaSp2-like protein.
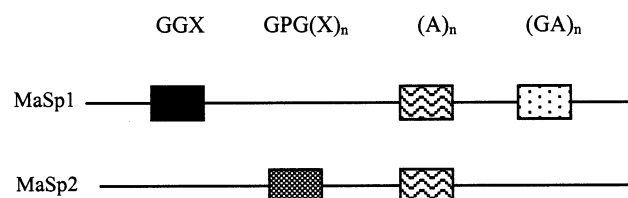

Figure 4. Structural motifs found in MA silk of *Latrodectus hesperus*.[13] MaSp1 and MaSp2 represent the proteins that comprise the major ampullate silk. The boxes represent modules that are found in silk, without respect to their actual physical positioning within the silk protein. For example, MaSp1 contains $(GA)_n$, $(A)_n$, and GGX motifs, whereas MaSp2 contains $GPG(X)_n$ and $(A)_n$ motifs but lacks GA elements.

ExPASy (Expert Protein Analysis System) and the proteins were analyzed using the computer program BLAST (Basic Local Alignment Search Tool). Two recombinant vectors carried cDNAs encoding proteins similar to reported spidroins. Both cDNAs encode partial length MaSp-like proteins, one encoding a 132 amino acid (aa) protein sharing homology to MaSp1 and one encoding a 140 aa protein with similarity to MaSp2 (see Figure 3). These proteins likely correspond to the two large molecular weight proteins observed by sodium dodecyl sulfate polyacrylamide gel electrophoresis (SDS−PAGE) from black widow MA silk.[16] The predicted primary sequence of the *L. hesperus* MA silk proteins identified in this study fits the proposed nomenclature of other MaSp proteins (see Figures 3 and 4). Furthermore, analysis of the primary sequence of the *L. hesperus* MaSp-like proteins demonstrated that these spidroins contain consensus ensemble repeats resembling MA silks from *Nephila* and *Araneus* (see Figure 5).

Overall, these two newly isolated cDNAs from *L. hesperus* contain motifs similar to other MA silks from other species. One cDNA encodes a silk protein homologous to MaSp1, containing GGX, GA, and polyalanine stretches, whereas the other cDNA encodes a protein with features more similar to MaSp2, containing $GPG(X)_n$ motifs as well as polyalanine stretches. Analysis of the primary sequence of *L. hesperus* MA silk clearly demonstrates that MA silk from cobweb
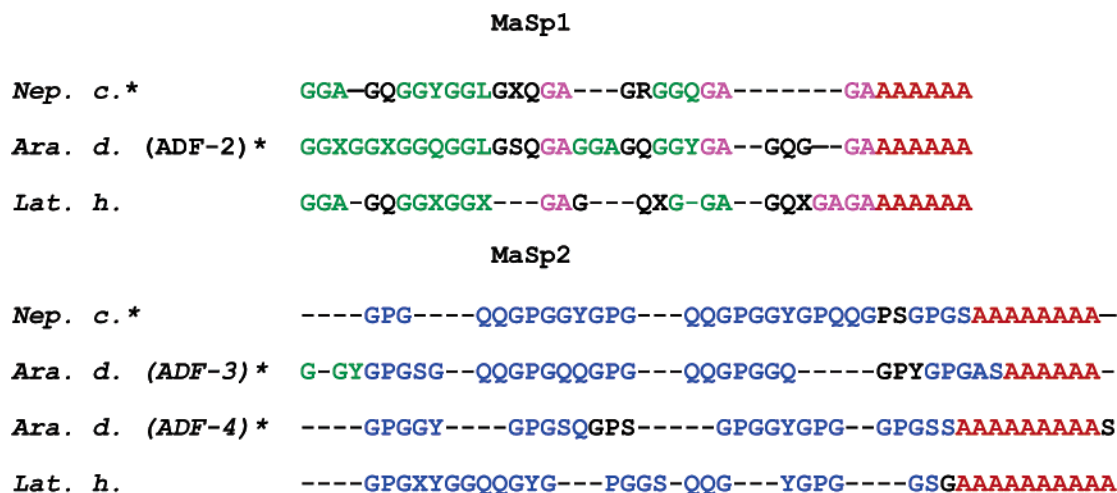
MaSp1

```
Nep. c.*          GGA—GQGGYGGLGXQGA---GRGGQGA-------GAAAAAAA

Ara. d. (ADF-2)*  GGXGGXGGQGGLGSQGAGGAGQGGYGA--GQG--GAAAAAAA

Lat. h.           GGA-GQGGXGGX---GAG---QXG-GA--GQXGAGAAAAAA
```

MaSp2

```
Nep. c.*          ----GPG----QQGPGGYGPG---QQGPGGYGPQQGPSGPGSAAAAAAAAA—

Ara. d. (ADF-3)*  G-GYGPGSG--QQGPGQQGPG---QQGPGGQ-----GPYGPGASAAAAAA-

Ara. d. (ADF-4)*  ----GPGGY----GPGSQGPS-----GPGGYGPG--GPGSSAAAAAAAAAS

Lat. h.           ----GPGXYGGQQGYG---PGGS-QQG---YGPG----GSGAAAAAAAAAA
```

Figure 5. Consensus ensemble repeat units for three araneoid fibroin ortholog groups. The consensus repeat for MaSp1-like and MaSp2-like proteins has been previously defined.[13] Single letter symbols representing the twenty amino acids are used and GGX, GA, A$_n$, and GPG(X)$_n$ motifs are indicated in green, pink, red, and blue, respectively. Dashes indicate gaps inserted into the alignments of ensemble repeat units for MaSp1 and MaSp2. Abbreviations are as follows: *Nep. c.*, *Nephila clavipes*; *Ara. d.*, *Araneus diadematus*; *Lat. h.*, *Latrodectus hesperus*. The symbol * indicates previously published sequence.[13,21,36] The previous designations for *Araneus diadematus* fibroins are shown in parentheses (ADF-2, ADF-3, and ADF-4). The letter X indicates that variability was often observed with respect to the amino acid at this position.

spiders contains the four motifs found (e.g., GGX, GA, GPG-(X)$_n$, and polyalanine modules) in MA silk from orb web spiders. However, closer analysis of the primary sequence of the MA silks from *L. hesperus* does demonstrate clear differences with respect to certain amino acids found within their predicted consensus ensemble repeats relative to *Nephila* and *Araneus*. These differences likely contribute, in part, to the observed mechanical property differences among MA silks.

In summary, we have studied the major ampullate silk from the cobweb building spider *L. hesperus* and have compared this silk to the MA silk from orb-web building spiders. Each of these major ampullate silks is used to support the weight of the spider as it hangs from the dragline. Orb web spiders also use MA silk as a structural element in their webs; however, no application has been observed for MA silk in the cobweb. Throughout our study, we see much greater similarity among the MA silks of spiders, even of those that construct different web types, than among previously studied silks from different glands produced by the same species of spider. Our studies, therefore, lend credence to the idea that MA silk has been optimized to perform the function of supporting the weight of the spider as it hangs. It is this function that ultimately determines the properties of major ampullate silk, not the species to which the spider belongs or the method of prey capture used by the spider.

References and Notes

(1) Vollrath, F.; Knight, D. P. *Nature* **2001**, *410*, 541−548.

(2) Gosline, J. M.; Guerette, P. A.; Ortlepp, C. S.; Savage, K. N. *J. Exp. Biol.* **1999**, *202*, 3295−3303.

(3) Xu, M.; Lewis, R. L. *Proc. Natl. Acad. Sci., U.S.A.* **1990**, *87*, 7120−7124.

(4) Hayashi, C. Y.; Shipley, N. H.; Lewis, R. L. *Int. J. Biol. Macromol.* **1991**, *24*, 271−275.

(5) Lombardi, S. J.; Kaplan, D. L. *J. Arachnol.* **1990**, *18*, 297−306.

(6) Andersen, S. O. *Comp. Biochem. Physiol.* **1970**, *35*, 705−711.

(7) Simmons, A. H.; Michal, C. A.; Jelinski, L. W. *Science* **1996**, *271*, 84−87.

(8) Kummerlen, J.; van Beek, J. D.; Vollrath, F.; Meier, B. H. *Macromolecules* **1996**, *29*, 2920−2928.

(9) van Beek, J. D.; Hess, S.; Vollrath, F.; Meier, B. H. *Proc. Natl. Acad. Sci.* **2002**, *99*, 10266−10271.

(10) Kovoor, J. In *Ecophysiology of Spiders*; Nentwig, W., Ed.; Springer-Verlag: New York, 1987; Vol. B, pp 161−186.

(11) Foelix, R. F. *Biology of Spiders*; Oxford University Press: New York, 1996.

(12) Kohler, T.; Vollrath, F. *J. Exp. Zool.* **1995**, *271*, 1−17.

(13) Gatesy, J.; Hayashi, C.; Motriuk, D.; Wood, J.; Lewis, R. *Science* **2001**, *291*, 2603−2605.

(14) Griswald, C. E.; Coddington, J. A.; Hormiga, G.; Scharff, N. *Zool. J. Linnean Soc.* **1998**, *123*, 1−99.

(15) Moore, A. M. F.; Tran, K. *Int. J. Biol. Macromol.* **1991**, *24*, 277−282.

(16) Botham, C. A.; Lopez, Y.; Moore, A. M. F. *J. Exp. Biol.* accepted.

(17) Casem, M. L.; Turner, D.; Houchin, K. *Int. J. Biol. Macromol.* **1991**, *24*, 103−108.

(18) Spagna, J. C.; Moore, A. M. F. *Pan-Pacific Entomol.* **1998**, *74*, 210.

(19) Work, R. W.; Emerson, P. D. *J. Arachnol.* **1982**, *10*, 1−10.

(20) Hinman, M. B.; Jones, J. A.; Lewis, R. A. *Trends Biotechnol.* **2000**, *18*, 374−379.

(21) Guerette, P. A.; Ginzinger, D. G.; Weber, B. H. F.; Gosline, J. M. *Science* **1996**, *272*.

(22) Madsen, B.; Shaoa, Z. Z.; Vollrath, F. *Int. J. Biol. Macromol.* **1991**, *24*, 301−306.

(23) Stauffer, S. L.; Coguill, S. L.; Lewis, R. V. *J. Arachnol.* **1994**, *22*, 5−11.

(24) Viney, C. In *Structural Biological Materials: Design and Structure−Property Relations*; Elices, M., Ed.; Pergamon Press: New York, 2000; pp 293−333.

(25) Work, R. W. *Text. J. Res.* **1976**, *46*, 485−492.

(26) Garrido, M. A.; Elices, M.; VIney, C.; Pérez-Rigueiro, J. *Polymer* **2002**, *43*, 4495−4502.

(27) Denny, M. *J. Exp. Biol.* **1976**, *65*, 483−506.

(28) Saito, H. *Magn. Reson. Chem.* **1986**, *24*, 835−852.

(29) Yang, Z.; Liivak, O.; Seidel, A.; LaVerde, G.; Zax, D. B.; Jelinski, L. W. *J. Am. Chem. Soc.* **2000**, *12*, 9019−9025.

(30) Asakura, T.; Watanabe, Y.; Uchida, A.; Minagawa, H. *Macromolecules* **1984**, *17*, 1075−1081.

(31) Wishart, D. S.; Sykes, B. D. *J. Biomol. NMR* **1994**, *4*, 171−180.

(32) Saito, H.; Iwanaga, Y.; Tabeta, R.; Narita, M.; Asakura, T. *Chem. Lett.* **1983**, 427−430.

(33) Simmons, A.; Ray, E.; Jelinski, L. W. *Macromolecules* **1994**, *27*, 5235−5237.

(34) Hijirida, D. H.; Do, K. G.; Michal, C.; Wong, S.; Zax, D.; Jelinski, L. W. *Biophys. J.* **1996**, *71*, 3442−3447.

(35) Liivak, O.; Flores, A.; Lewis, R.; Jelinski, L. *Macromolecules* **1997**, *30*, 7127−7130.

(36) Hayashi, C. Y.; Lewis, R. L. *J. Mol. Biol.* **1998**, *275*, 773−784.